

Importance of Co 3d electron correlation in a Ce-based Kondo lattice, Ce₂CoSi₃

Swapnil Patil, Sudhir Pandey, V. R. R. Medicherla, R. S. Singh, R. Bindu, E. V. Sampathkumaran, and Kalobaran Maiti*

*Department of Condensed Matter Physics and Materials Science,
Tata Institute of Fundamental Research, Homi Bhabha Road, Colaba, Mumbai 400005, India*

(Dated: November 9, 2018)

We study the role of electron correlations among Co 3d electrons contributing to the conduction band of a Kondo lattice compound, Ce₂CoSi₃, using high resolution photoemission spectroscopy and *ab initio* band structure calculations. Experimental results reveal signature of Ce 4f states derived Kondo resonance feature at the Fermi level and dominance of Co 3d contributions at higher binding energies in the valence band. The line shape of the experimental Co 3d band is found to be significantly different from that obtained from the band structure calculations within the local density approximations. Consideration of electron-electron Coulomb repulsion among Co 3d electrons leads to a better representation of experimental results. The correlation strength among Co 3d electrons is found to be about 3 eV. Signature of electron correlation induced satellite feature is also observed in the Co 2p core level spectrum. Thus, these results demonstrate the importance of the electron correlation among conduction electrons to derive the microscopic description of such Kondo systems.

PACS numbers: 75.20.Hr, 71.27.+a, 71.28.+d, 71.15.Mb

I. INTRODUCTION

Study of Ce-intermetallics have drawn significant attention during past few decades due to the observation of many unusual properties such as valence fluctuations, Kondo screening, heavy fermion superconductivity in these systems. Such properties arise due to the proximity of Ce 4f level to the Fermi level leading to strong hybridization between the Ce 4f states and the conduction electronic states.¹ A lot of success has been achieved to describe these systems within the Anderson impurity models. Here, the parameters defining the hybridization between 4f states and valence electronic states are often estimated using band structure calculations based on local density approximations (LDA).^{2,3,4,5} However, the scenario can be significantly different if these materials contain transition metals; the d electrons contribute to the conduction band and the finite correlation strength among them leads to non-applicability of the band structure results within LDA.

Here, we report the results of our investigations on the electronic structure of Ce₂CoSi₃ using high resolution photoemission spectroscopy and *ab initio* band structure calculations. Ce₂CoSi₃ crystallizes in a AlB₂ derived hexagonal structure (space group *P6/mmm*) and is a mixed valent (Kondo lattice) compound.^{6,7,8} The electrical transport measurements revealed temperature dependence⁸ typical of a mixed valent system.⁹ No signature of magnetic ordering was observed in the magnetic susceptibility measurements down to 0.5 K.⁸ Interestingly, gradual substitution of Rh at Co sites leads to plethora of interesting features due to increasing dominance of indirect exchange interaction.⁸ For example, $x = 0.6$ composition in Ce₂Rh_{1-x}Co_xSi₃ exhibits quantum critical behavior. Intermediate compositions having higher Rh concentration exhibit signature of spin den-

sity wave (SDW) state.⁸ Thus, the d electronic states corresponding to the transition metals plays a key role in determining the electronic properties in this interesting class of compounds. Therefore, Ce₂CoSi₃ could be one of the ideal ones where the correlation among the electronic states other than Ce 4f states is important.

High energy resolution employed in our measurements enabled us to reveal Kondo-resonance feature and the corresponding spin orbit satellite. The comparison of the experimental spectra and the calculated ones indicate that the correlation strength among Co 3d electrons is strong (~ 3 eV). The contribution of the Co 3d partial density of states (PDOS) is small in the vicinity of the Fermi level, where Ce 4f contributions are dominant.

II. EXPERIMENTAL DETAILS

Ce₂CoSi₃ was prepared by melting together stoichiometric amounts of high purity (> 99.9%) Ce, Co and Si in an arc furnace. The single phase was confirmed by the absence of impurity peaks in the x-ray diffraction pattern. The specimen was further characterized by scanning electron microscopic measurements and energy dispersive x-ray analysis.⁸ The photoemission measurements were performed using a Gammatdata Scienta SES2002 analyzer and monochromatic laboratory photon sources. The energy resolutions were set to 0.4 eV, 5 meV and 5 meV at Al *K* α (1486.6 eV), He II α (40.8 eV) and He I α (21.2 eV) photon energies, respectively. The base pressure in the vacuum chamber was 3×10^{-11} torr. The temperatures variation down to 20 K was achieved by an open cycle He cryostat (LT-3M, Advanced Research Systems, USA). The sample surface was cleaned by *in situ* scraping using a diamond file and the surface cleanliness was ensured by the absence of O 1s and C 1s features

in the x -ray photoelectron (XP) spectra and the absence of impurity features in the binding energy range of 5-6 eV in the ultraviolet photoelectron (UP) spectra. The reproducibility of the spectra was confirmed after each trial of cleaning process.

III. CALCULATIONAL DETAILS

The electronic band structure of Ce_2CoSi_3 was calculated using *state-of-the-art* full potential linearized augmented plane wave (FLAPW) method using WIEN2k software¹⁰ within the local density approximations, LDA. The convergence for different calculations were achieved considering 512 k points within the first Brillouin zone. The error bar for the energy convergence was set to < 0.2 meV per formula unit (fu). In every case, the charge convergence was achieved to be less than 10^{-3} electronic charge. The lattice constants used in these calculations are determined from the x -ray diffraction patterns considering AlB_2 derived hexagonal structure and are found to be $a = 8.104$ Å and $c = 4.197$ Å.⁶ The muffin-tin radii (R_{MT}) for Ce, Co and Si were set to 2.5 a.u., 2.28 a.u. and 2.02 a.u., respectively.

IV. RESULTS AND DISCUSSIONS

The valence band in Ce_2CoSi_3 consists of Ce $5d$, Ce $4f$, Co $3d$ and Si $3p$ electronic states. Since the transition probability of the photoelectrons in the photo-excitation process strongly depends on the excitation energies, a comparison of the photoemission spectra collected at different excitation energies would help to identify experimentally the character of various features constituting the valence band. In Fig. 1(a), we show the valence band spectra collected at 20 K using Al $K\alpha$ photon energy and the He $\text{II}\alpha$ and He $\text{I}\alpha$ spectra are shown in Fig. 1(b). Each spectrum exhibits two distinct features, A and B at about 1 eV and 2.3 eV binding energies, respectively. Interestingly, the relative intensity of these features does not change with such a large change in photon energies. This is unusual as the photoemission cross sections corresponding to Ce $5d$, Ce $4f$, Co $3d$ and Si $3p$ electronic states have significantly different excitation energy dependence.¹¹

To verify the change in lineshape with better clarity, we have broadened the He II spectrum by convoluting a Gaussian of full width at half maximum (FWHM) = 0.4 eV to make the resolution broadening comparable to that of the XP spectrum. The broadened spectrum is shown by solid line superimposed over the XP spectrum in Fig. 1(a). The lineshapes of both the spectra are almost identical. In Fig. 1(b), the He I and He II spectra are superimposed over each other to investigate the change in lineshape when the energy resolution broadening is the same (~ 5 meV). The spectra in the binding energy range beyond 1 eV are found to be almost iden-

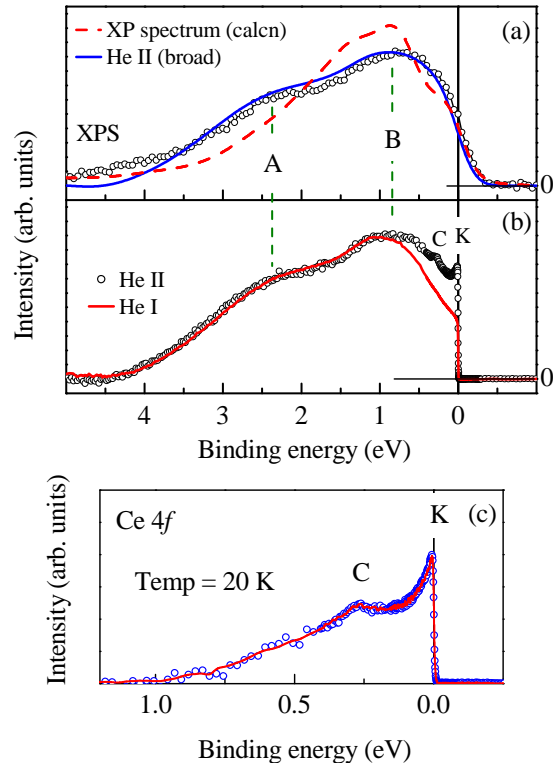


FIG. 1: Valence band spectra collected using (a) Al $K\alpha$ (XPS), and (b) He II and He I excitation energies. The solid line in (a) represents the broadened He II spectrum to take into account the energy resolution corresponding to XP spectrum. Dashed line represent the calculated XP spectrum. (c) The Ce $4f$ spectral function obtained by subtracting He I spectrum from the He II spectrum.

tical. All these observations suggest that the binding energy range > 1 eV of the valence band is dominantly contributed by one kind of electronic states.

The intensity close to the Fermi level, ϵ_F , exhibit significantly different behavior as a function of excitation energy (see Fig. 1(b)). He II spectrum exhibits large intensity and two distinct features C and K near ϵ_F , which are not visible in the other spectra. The high energy resolution employed in the He I and He II measurements helped to resolve distinct signature of the features in the vicinity of ϵ_F . The photoemission cross section for Ce $4f$ states at He II excitation energy is about 3 times larger than that at He I photon energy while it is almost the same for Si $3p$ states and double for Co $3d$ states.¹¹ Thus, the features C and K can be attributed to the photoemission signal primarily from the Ce $4f$ states. We have subtracted the He I spectrum from the He II spectrum to delineate the Ce $4f$ contributions. The subtracted spectrum representing Ce $4f$ band is shown

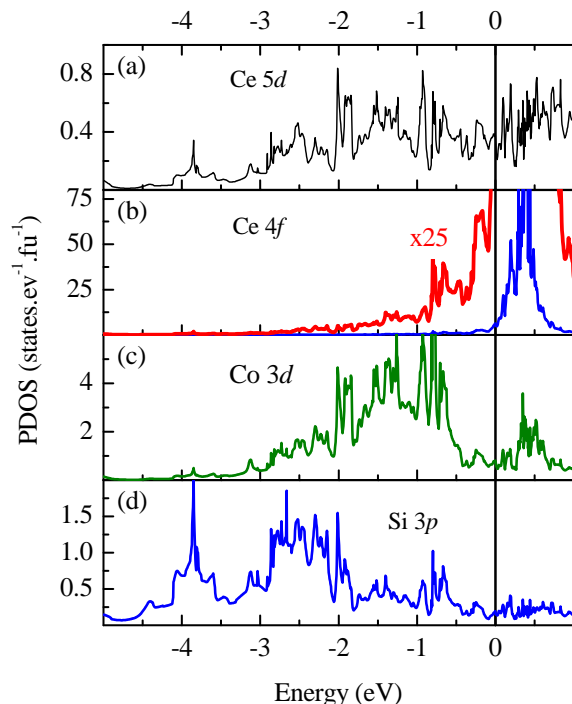


FIG. 2: Calculated (a) Ce 5d partial density of states (PDOS), (b) Ce 4f PDOS, (c) Co 3d PDOS and (d) Si 3p PDOS. The thick solid line in (b) represents the Ce 4f PDOS rescaled by 25 times to show the weak intensities at lower energies.

in Fig. 1(c). The distinct features, C and K corresponding to the spin orbit satellite of the Abrikosov-Suhl resonance (ASR) and the main peak of ASR, respectively, could clearly be identified.¹²

In order to verify the character of the features theoretically, we have calculated the electronic band structure using FLAPW method. The calculated partial density of states (PDOS) are shown in Fig. 2. The dominant contribution in this energy range arises from the Ce 5d, Ce 4f, Co 3d and Si 3p PDOS as shown in Fig. 2(a), 2(b), 2(c) and 2(d) respectively. All the other contributions are negligible in this energy range. Evidently, Ce 5d contributions are small and almost equally distributed over the whole energy range shown. Ce 4f band is intense and narrow as expected. In order to provide clarity, we have rescaled the Ce 4f partial density of states (PDOS) by 25 times and shown by thick solid line in Fig. 2(b). Clearly, the 4f PDOS contribute essentially in the vicinity of the Fermi level (< 1 eV binding energy). The intensity of Ce 4f band is significantly weak at higher binding energies. This is consistent with the observation in Fig. 1(b). Co 3d states also have finite contributions in this energy range due to the hybridization between Co 3d and Ce 4f states.

Co 3d and Si 3p electronic states also exhibit significant hybridization effect and appears dominantly in the binding energy range larger than 0.5 eV. The bonding states contribute in the energy range higher than 2 eV binding energy, where the Si 3p PDOS has large contributions. The antibonding features appear in the energy range 0.5 to 2 eV, where Co 3d contributions are dominant. This suggests that the feature B in Fig. 1 has dominant Co 3d character and the intensities corresponding to Si 3p photoemission contribute to feature A. The dominance of Co 3d contributions in this whole energy range shown presumably leads to unchanged spectral lineshape with the change in photon energy as observed in Fig 1(a) and 1(b).

In order to compare the experimental spectrum with the calculated results, we have calculated the XP spectrum in the following way: the Ce 5d, Ce 4f, Co 3d and Si 3p PDOS per formula unit were multiplied by the corresponding photoemission cross sections at Al $K\alpha$ energy. The sum of all these contributions was convoluted by the Fermi distribution function at 20 K and broadened by the Lorentzian function to account for the photo-hole lifetime broadening. The resolution broadening is introduced via further broadening of the spectrum by a gaussian function of FWHM = 0.4 eV. The calculated spectrum is shown by dashed line in Fig. 1(a) after normalizing by the total integrated area under the curve. The intensities near ϵ_F in the experimental spectrum appears to be captured reasonably well in the calculated spectra.

In the higher binding energy region; the intensity around 1 eV is overestimated and that around 2.5 eV is underestimated. Since this energy range contains dominant contribution from the Co 3d states, it naturally indicates that Co 3d PDOS region is not well described and correlations among Co 3d electrons may be important in determining the electronic structure in this energy range. In order to verify this, we have calculated the electronic density of states considering finite electron correlation, U_{dd} , among Co 3d electrons. The spectral functions corresponding to different U_{dd} values are calculated from the LDA+ U results following the procedure described above.

The lines in Fig. 3 represent the spectral functions for different U_{dd} values which are superimposed on the experimental XP spectrum represented by open circles. In Fig. 3(a) we show the calculated spectra without Ce 4f contributions and the ones including Ce 4f contributions are shown in Fig. 3(b). It is evident from the figure that the signature of the feature around 2.3 eV (feature B) becomes more and more prominent with the increase in U_{dd} . Subsequently, the intensity of feature A reduces. Thus, the feature B can be attributed to the photoemission signal from electron correlation induced Co 3d bands (lower Hubbard band) in addition to the Si 3p contributions. It is clear that the calculated spectral functions corresponding to $U_{dd} \sim 3$ eV is closest to the experimental spectrum compared to all other cases. For higher values of U_{dd} , the correlation induced feature becomes stronger and appears at higher binding energies.

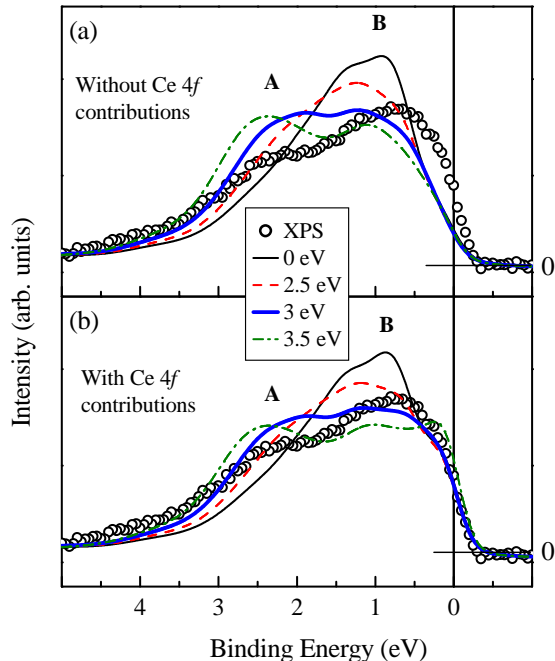


FIG. 3: X-ray photoemission valence band spectrum (open circles) is compared with the calculated spectral functions corresponding to different U_{dd} -values. (a) The calculated spectral functions without Ce $4f$ contributions. (b) The calculated spectral functions contains Ce $4f$ contributions. Clearly, the results in (b) provide better description than that in (a) revealing signature of Ce $4f$ contributions in the vicinity of the Fermi level.

The comparison of Fig. 3(a) and 3(b) establishes that the intensities near ϵ_F essentially arise due to the photoemission from the occupied part of the Ce $4f$ band. Co $3d$ contributions are small in this energy range and the Co $3d$ correlation induced effects has negligible influence on the spectral intensity at ϵ_F . Consideration of Ce $4f$ bands in the spectral function calculation leads to a better description of the spectral intensities at the Fermi level. In order to investigate the role of correlation among Ce $4f$ electrons in the electronic structure, we show the Ce $4f$ PDOS calculated for $U_{ff} = 0$ and 4 eV in Fig. 4. The unoccupied part of the spectral function exhibits large redistribution. The occupied part exhibits small change in lineshape as shown with better clarity in Fig. 4(b). The peak at ϵ_F enhances and subsequently, the intensity between 0 and -0.3 eV energies reduces. The rest of the occupied part remains almost unchanged.

The signature of electron correlations can also be observed in the Co $2p$ core level spectra.¹³ In Fig. 5, we show the Co $2p$ spectrum collected at 20 K using Al $K\alpha$ radiation. The spectrum consists of two spin orbit split

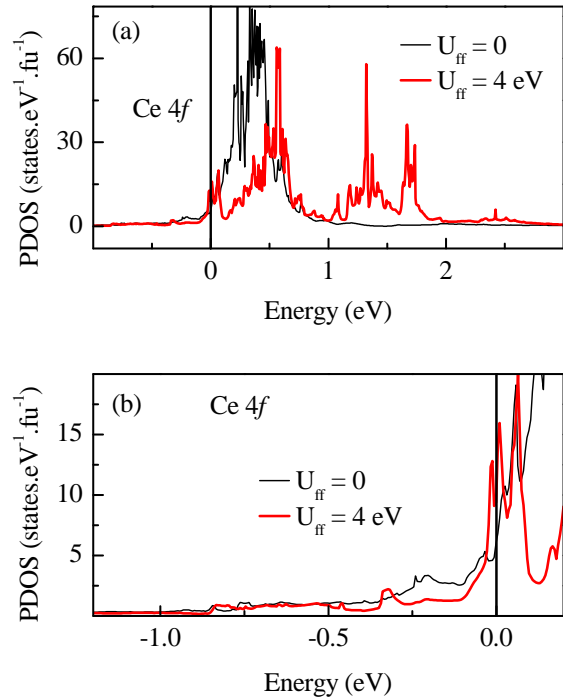


FIG. 4: Calculated Ce $4f$ partial density of states for different electron correlation strength, U_{ff} among Ce $4f$ electrons. The results corresponding to the whole energy range is shown in (a) and that near Fermi level is shown in (b).

features Co $2p_{3/2}$ and Co $2p_{1/2}$ at 778 eV and 792.9 eV binding energies, respectively (energy separation of about 14.9 eV). These binding energies are identical to those found in elemental Co metals.^{14,15} This indicates that the valence state of Co is very similar to the elemental Co metals. In addition, every spin orbit split feature exhibits a weak but distinct shoulder at higher binding energies. This has been shown more clearly by rescaling and shifting this energy region in the same figure. The energy separation between the main peak and the satellite is about 4 eV. Finite intensity of the satellite feature again establishes the presence of electronic correlations among Co $3d$ electrons.¹³ Thus, our results establish that the electron correlation strength among Co $3d$ electrons are significant and needs consideration to describe the electronic structure of these systems.

V. CONCLUSIONS

In summary, we have studied the electronic structure of Ce₂CoSi₃ using high resolution photoemission spectroscopy and *ab initio* band structure calculations. The experimental results indicate the dominance of Co $3d$ contributions in the valence band. Si $3p$ states appear at

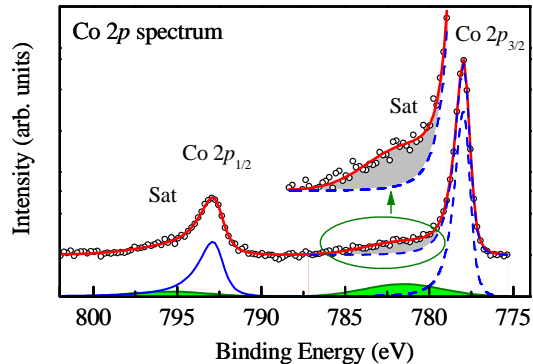


FIG. 5: Co $2p$ spectrum (open circles) exhibiting distinct signature of main and satellite peaks. The satellite intensity is shown by shaded region. Solid line passing through the experimental data represents the fit comprising of a main peak (dashed line) and a satellite (shaded peak).

higher binding energies (2 - 3 eV). The Ce $4f$ contributions appear essentially in the vicinity of the Fermi level. High resolution employed in this study helped to probe the Kondo resonance feature appearing at the Fermi level. Although the contribution of the Co $3d$ states at ϵ_F is weak, Co $3d$ states are found to be hybridized with the Ce $4f$ states. The comparison of the experimental results with the calculated ones indicate that Co $3d$ electrons are strongly correlated. These results thus, establish that in addition to the electron correlations among Ce $4f$ electrons, correlation among d electrons needs to be considered to derive the electronic properties of these systems.

VI. ACKNOWLEDGEMENTS

One of the authors S.P., thanks the Council of Scientific and Industrial Research, Government of India for financial support.

* Electronic mail: kbmaiti@tifr.res.in

- ¹ N. B. Brandt and V. V. Moshchalkov, *Advances in Physics* **33**, 373 (1984).
- ² John M. Willis and Bernard R. Cooper, *Phys. Rev. B* **36**, 3809 (1987).
- ³ O. Gunnarsson and O. Jepsen, *Phys. Rev. B* **38**, 3568 (1988).
- ⁴ O. Gunnarsson, O. K. Andersen, O. Jepsen and J. Zaanen, *Phys. Rev. B* **39**, 1708 (1989).
- ⁵ O. Gunnarsson and K. Schönhammer, *Phys. Rev. B* **40**, 4160 (1989).
- ⁶ R. A. Gordon, C. J. Warren, M. G. Alexander, F. J. DiSalvo and R. Pöttgen, *J. Alloys Compounds* **248**, 24 (1997).
- ⁷ Subham Majumdar, M. Mahesh Kumar, R. Mallik and E. V. Sampathkumaran, *Solid State Comm.* **110**, 509 (1999).
- ⁸ Swapnil Patil, Kartik K. Iyer, K. Maiti and E. V. Sampathkumaran, *Phys. Rev. B* **77**, 094443 (2008); Swapnil Patil, Kartik K. Iyer, K. Maiti and E. V. Sampathkumaran, condmat-0803.0652.

- ⁹ J. M. Lawrence, P. S. Riseborough and R. D. Parks, *Rep. Prog. Phys.* **44**, 1 (1981).
- ¹⁰ P. Blaha, K. Schwarz, G.K.H. Madsen, D. Kvasnicka, and J. Luitz, **WIEN2k**, An Augmented Plane Wave + Local Orbitals Program for Calculating Crystal Properties (Karlheinz Schwarz, Techn. Universität Wien, Austria), 2001. ISBN 3-9501031-1-2.
- ¹¹ J.J. Yeh and I. Lindau, *At. Data Nucl. Data Tables* **32**, 1 (1985).
- ¹² D. Ehm, S. Hüfner, F. Reinert, J. Kroha, P. Wölfle, O. Stockert, C. Geibel and H. v. Löhneysen, *Phys. Rev. B* **76**, 045117 (2007).
- ¹³ Masatoshi Imada, Atsushi Fujimori and Yoshinori Tokura, *Rev. Mod. Phys.* **70**, 1039 (1998).
- ¹⁴ Krishna G. Nath, Y. Haruyama and T. Kinoshita, *Phys. Rev. B* **64**, 245417 (2001).
- ¹⁵ C. M. Schneider, U. Pracht, W. Kuch, A. Chassé and J. Kirschner, *Phys. Rev. B* **54**, R15618 (1996).